BEST AVAILABLE IMAGES

Defective images within this document are accurate representations of the original documents submitted by the applicant.

Defects in the images may include (but are not limited to):

- BLACK BORDERS
- TEXT CUT OFF AT TOP, BOTTOM OR SIDES
- FADED TEXT
- ILLEGIBLE TEXT
- SKEWED/SLANTED IMAGES
- COLORED PHOTOS
- BLACK OR VERY BLACK AND WHITE DARK PHOTOS
- GRAY SCALE DOCUMENTS

IMAGES ARE BEST AVAILABLE COPY.

As rescanning documents *will not* correct images, please do not report the images to the Image Problem Mailbox.

Heparanase expression in invasive trophoblasts and acute vascular damage

Laurie A.Dempsey[2], Timothy B.Plummer[2], Sarah A.Coombes[2] and Jeffrey L.Platt[1,2,3,4]

[2]Departments of [2]Surgery, [3]Immunology, and [4]Pediatrics, Mayo Clinic, Rochester, MN 55905, USA

Received on July 6, 1999; revised on November 16, 1999; accepted on November 16, 1999

Heparan sulfate proteoglycans play a pivotal role in tissue function, development, inflammation, and immunity. We have identified a novel cDNA encoding human heparanase, an enzyme thought to cleave heparan sulfate in physiology and disease, and have located the *HEP* gene on human chromosome 4q21. Monoclonal antibodies against human heparanase located the enzyme along invasive extravillous trophoblasts of human placenta and along endothelial cells in organ xenografts targeted by hyperacute rejection, both sites of heparan sulfate digestion. Heparanase deposition was evident in arterial walls in normal tissues; however, vascular heparan sulfate cleavage was coincident with heparanase enzyme during inflammatory episodes. These findings suggest that heparanase elaboration and control of catalytic activity may contribute to the development and pathogenesis of vascular disease and suggest that heparanase intervention might be a useful therapeutic target.

Key words: heparanase/heparan sulfate/hyperacute rejection/placenta/xenografts

Introduction

Heparan sulfate proteoglycans are found on cell surfaces and in extracellular matrices where they participate in critical molecular interactions influencing cell adhesion, cell fate, regulation of vascular function, lipoprotein metabolism, and immune responses (Kjellen and Lindahl, 1991; Ihrcke *et al.*, 1993; Rosenberg *et al.*, 1997; Lindahl *et al.*, 1998). In a broad sense heparan sulfate might be thought to establish and maintain the differentiated state of cells and tissues (Platt *et al.*, 1990a). Composed of alternating glucosamine and hexuronic acid residues modified by sulfation and epimerization, heparan sulfate glycosaminoglycans display an extraordinary diversity of potential binding ligands (Salmivirta *et al.*, 1996; Rosenberg *et al.*, 1997). Heparan sulfate is thought to promote the anticoagulant, antioxidant and barrier properties of blood vessel endothelium by sequestering and activating enzymes and regulatory molecules, preventing the formation of occlusive vascular thrombin and protecting against proteolytic or oxidative damage (Vlodavsky *et al.*, 1992; Rosenberg *et al.*, 1997; Stringer and Gallagher, 1997). Heparan sulfate tethers chemokines that activate and direct the migration of lymphocytes to antigen-presenting cells (Kim and Broxmeyer, 1999). Heparan sulfate metabolism may also be critical in early extraembryonic tissues to allow blastocyst implantation and fetal growth and development (reviewed by Cross *et al.*, 1994; Carson *et al.*, 1998).

Besides contributing to tissue homeostasis and development, heparan sulfate metabolism may be linked to disease. During inflammation, the extravasation of leukocytes is linked to loss of heparan sulfate from endothelial cells and extracellular matrices (Naparstek *et al.*, 1984; Matzner *et al.*, 1985; Fridman *et al.*, 1987; Shimada and Ozawa, 1987; Ishai-Michaeli *et al.*, 1990). Tumor cell metastatic potential also correlates with the ability to degrade heparan sulfate proteoglycans (Nakajima *et al.*, 1988; Vlodavsky *et al.*, 1992). Heparanase inhibitors dramatically reduce the incidence of lung metastases following injection of metastatic tumor cells in mice (Nakajima *et al.*, 1983; Vlodavsky *et al.*, 1988; Villanueva *et al.*, 1989). Tumor angiogenesis may be promoted by releasing heparan sulfate-associated growth factors sequestered in the underlying extracellular matrix, amplifying the effect of heparan sulfate degradation (Vlodavsky *et al.*, 1988; Weiss *et al.*, 1988; Ishai-Michaeli *et al.*, 1990). Immune cell interactions can be bolstered *in vitro* by heparan sulfate as shown by increasing T cell proliferation and cytotoxicity and by stimulating antigen-presenting cells (Wrenshall *et al.*, 1991, 1994).

Heparan sulfate proteoglycans might be shed from cells and tissues by one or more of four mechanisms: (1) proteolytic cleavage of the protein core, (2) phospholipase-mediated cleavage of a lipid anchor, (3) release of peripheral membrane proteoglycans by disruption of ionic interactions, and (4) cleavage of glycosaminoglycan chains by endoglycosidases (Brunner *et al.*, 1991; Bernfield *et al.*, 1992; Yanagishita, 1992; Yanagishita and Hascall, 1992; Ihrcke and Platt, 1996). Of these, glycosaminoglycan cleavage would be expected to have the most profound impact on tissue physiology, since it is predominantly the glycosaminoglycan chains that confer biological function to heparan sulfate proteoglycans (Salmivirta *et al.*, 1996; Stringer and Gallagher, 1997; Lindahl *et al.*, 1998). Activated platelets can release heparanase at sites of inflammation (Oosta *et al.*, 1982). Because heparan sulfate plays a critical role in maintaining vascular integrity and in development, we postulated that elaboration of heparanase might be tightly regulated. Platelet heparanase is inactive at physiological pH, but becomes highly active at acidic pH, as occurs during inflammation (Gilat *et al.*, 1995; Ihrcke *et al.*, 1998). However, heparanase retains its ability to bind to

[1]To whom correspondence should be addressed at: 2–69 Medical Sciences Building, Mayo Clinic, Rochester, MN 55905

heparan sulfate molecules at physiological pH (Ihrcke *et al.*, 1998) and is, possibly, stored in extracellular domains.

Heparanase activity has been variously attributed to proteins of molecular mass ranging between 40–60 kDa (Freeman and Parish, 1998; Gonzalez-Stawinski *et al.*, 1999; Goshen *et al.*, 1996; Graham and Underwood, 1996; Sandbäck Pikas *et al.*, 1998), to a 9 kDa CXC chemokine CTAP-III (Hoogewerf *et al.*, 1995), or a 134 kDa endoglycosidase activity derived from platelets (Oosta *et al.*, 1982). The discrepancies regarding the identity of heparanase and the difficulty in obtaining pure heparanase preparations has precluded detailed mechanistic studies on the regulation of heparanase expression and activity. In this report, we have begun to characterize the contribution of heparanase in health and disease by identification of human heparanase cDNAs and the gene encoding human heparanase, and by localization of heparanase protein expression in normal tissues and in diseased organs.

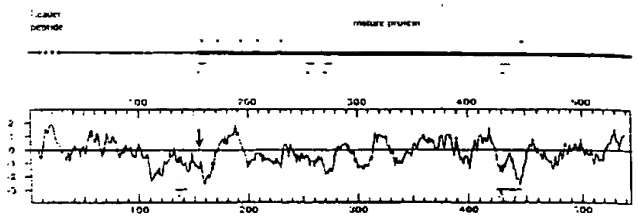

Fig. 1. Organization of human platelet heparanase protein. The deduced amino acid sequence predicts a protein of 61 kDa. Protein modification by cleavage and N-glycosylation generates the mature protein of 55 kDa. A schematic representation of the heparanase protein is shown above, which depicts the precursor N-terminal region (thin line) and peptide leader sequence, the mature protein (thick line) and clustered basic regions (+) which may contribute to heparan sulfate recognition and binding. Asterisks indicate putative N-glycosylation sites. The Kyte-Doolittle hydrophobicity plot of heparanase protein is shown. Immunizing peptides Hep-1, -2, and -3 used to generate anti-heparanase antibodies are depicted within the hydrophobicity plot.

Results

Identification of cDNAs encoding human heparanase

Based upon peptide sequence derived, as previously described, from the purified platelet enzyme (Gonzalez-Stawinski *et al.*, 1999), we identified several partial cDNAs encoding human heparanase by searching the translated GenBank dbEST database. We obtained the full-length heparanase cDNA sequence by performing 5′ RACE on human placental and megakaryoblast cDNAs. The 543 amino acid heparanase product was encoded by a 1632 nt open reading frame and has a predicted molecular weight of 61.168 Da. The heparanase cDNA terminated 27 nt downstream from the stop codon, which overlapped polyadenylation signal, and no instability elements were found in the 3′ untranslated region. Importantly, the heparanase-encoding EST sequences were selectively expressed in human malignancies, such as metastatic lung carcinomas and kidney and colon tumors, and also from ulcerative colitis colon samples, consistent with the notion that heparanase expression occurs in metastatic and inflammatory diseases.

The predicted heparanase amino acid sequence revealed several relevant features that are shown in Figure 1. BLAST searches of the protein database or translated nucleic acid databases failed to reveal any known protein of similar sequence. Hileman *et al.* (1998) and Cardin and Weintraub (1989) identified heparin- or heparan sulfate-binding protein consensus motifs XBBBXXBX and XBBXBX, thought to be important for ionic interactions with glycosaminoglycan ligands. Human heparanase contains two regions of clustered basic amino acids, 272–278 (PRRKTAKM) and 157–162 (QKKFKN), which conform to these binding motif patterns (Figure 1). The highly basic peptide KRRKLRV, amino acids 426–432, is also present in heparanase protein. Platelets release heparanase as a 55 kDa soluble enzyme, suggesting that protein processing may occur to produce the mature enzyme. Hulett *et al.* (1999) reported processing of the precursor heparanase between amino acids 157–158 to give the mature product. Six putative N-glycosylation sites are present in the heparanase conceptual sequence. We have shown, previously, that purified heparanase binds to Concanavalin A (Gonzalez-Stawinski *et al.*, 1999), suggesting that one or more glycosidation sites may be used *in vivo*.

Verification of the protein product using anti-heparanase antibodies

To confirm the identity of the heparanase cDNA and protein product we developed affinity-purified rabbit antibodies and mouse monoclonal antibodies and tested the ability of the antibodies to recognize native and denatured forms of platelet heparanase. Anti-heparanase antibodies were generated by immunizing mice and rabbits with the peptides KLRVYLH-CTNTDN (amino acid residues 430–442), CKYGSIPPD-VEEK (amino acids 128–140) and TKVLMASVQGSKRRK (amino acids 417–431) in the conceptual translated sequence, which were predicted to be solvent-accessible by the Kyte-Doolittle protein hydropathy algorithm (Kyte and Doolittle, 1982) (Figure 1). The highly basic peptide 1 epitope was found within one of the endoLysC peptides obtained from purified mature heparanase protein (Gonzalez-Stawinski *et al.*, 1999) and may comprise part of the heparan sulfate substrate binding site (Figure 1). Antibody specificity was confirmed by four lines of evidence. Affinity-purified rabbit polyclonal and murine monoclonal anti-heparanase antibodies recognized the native heparanase protein in ELISA assays, and binding was inhibited by the aforementioned synthetic peptide (Figure 2A). The affinity-purified rabbit antibody and several monoclonal antibodies also recognized denatured heparanase protein in western blots (Figure 2B). Antibody depletion by affinity-peptide chromatography using the immunizing peptide removed all antibodies reactive against the partially purified heparanase as assayed by ELISA and by immunostaining human placental tissue sections (not shown). Murine monoclonal anti-heparanase antibodies were tested for their ability to inhibit heparanase endoglycosidase activity in platelet extracts, which is a more stringent test of antigen recognition. To assess the effect of anti-heparanase antibody on enzyme activity, we preincubated platelet lysates in heparanase assay buffer (pH 6.5) with purified anti-heparanase antibodies and subsequently, assayed for endoglycosidase activity by incubation with ^{3}H-heparan sulfate covalently linked to Sepharose

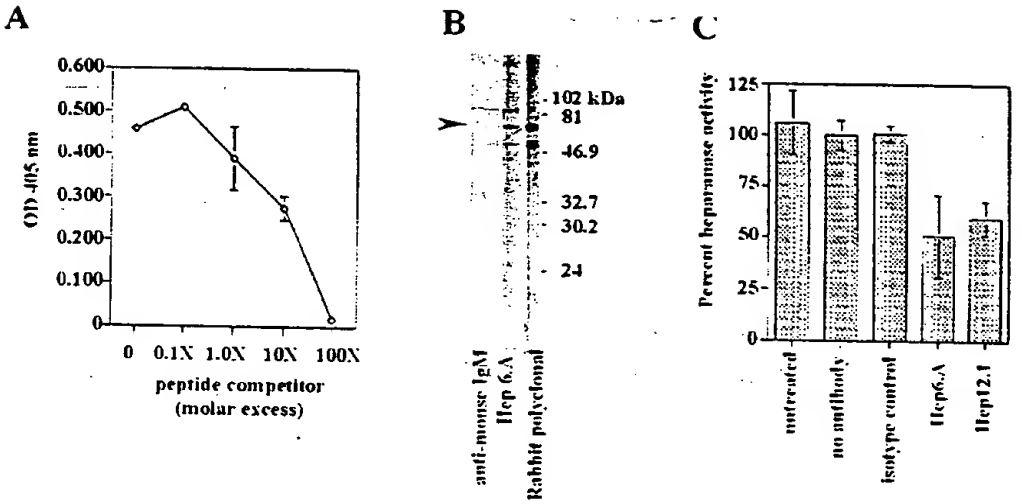

Fig. 2. Specificity of anti-heparanase antibodies. (A) Anti-heparanase recognition of native platelet heparanase can be blocked by excess peptide. ELISA dose-response curve showing the peptide KLRVYLHCTNTDN, inhibits recognition of partially-purified platelet heparanase by the anti-heparanase antibody Hep1.1A. (B) Western immunoblots demonstrate the specific recognition of a 55 kDa protein (arrowhead) in human platelet lysates by murine monoclonal, Hep6.A, or rabbit polyclonal anti-heparanase antibodies. Platelet proteins were electrophoresed through 10–20% denaturing gradient gels and blotted onto PVDF membranes, and probed using antibodies raised against the heparanase-specific peptide KLRVYLHCTNTDN. Detection of the immune complexes was performed using alkaline phosphatase-conjugated anti-mouse IgM or anti-rabbit IgG secondary antibodies. Goat anti-mouse IgM alone, anti-rabbit IgG (not shown), or rabbit preimmune serum (not shown) failed to detect the 55 kDa protein. Molecular mass markers are shown on the right. (C) Inhibition of heparanase endoglycosidase activity by anti-heparanase antibodies. Platelet lysates were pretreated with anti-heparanase antibodies Hep6A or Hep12.1, with an unrelated anti-complement factor C5 IgM antibody as an isotype control, in heparanase assay buffer at pH 6.5 for 3 h prior to the addition of ^{3}H-heparan sulfate-coupled Sepharose beads. Untreated platelet lysates were also assayed for heparanase activity. The release of ^{3}H-heparan sulfate into the supernatant was measured by scintillation counting and reported as the percent activity relative to the pretreated control without antibody. Assays were performed in triplicate and are representative of three independent experiments performed with different platelet extracts.

beads. Several independently-isolated anti-heparanase monoclonal antibodies, Hep6A and Hep12.1, reduced heparanase activity as measured by the release of ^{3}H-heparan sulfate to 51% or 60% of the no antibody-treated control, respectively (Figure 2C), whereas an antibody isotype control, 2C18, which recognizes unrelated complement factor C5, did not diminish heparanase activity. Heparanase activity released by human megakaryocyte cell line CHRF-288 was similarly reduced by preincubation with the anti-heparanase Hep6.A and Hep 12.1 monoclonal antibodies to less than 50% of the mock-treated or 2C18 controls (not shown). The failure of anti-heparanase antibodies to completely inhibit enzyme activity may reflect recognition of an epitope distinct from the active site. Alternatively, the inability to completely inhibit enzyme activity may reflect diminished binding of the antibodies at pH 6.5 owing to conformational change of the antibodies or protonation of the histidine residue in the antibody binding site of the heparanase protein.

Localization of the human heparanase gene

To identify the gene encoding heparanase, a human chromosomal library composed of P1-derived artificial chromosomes (1×10^5 clone array with an average insert size of 120 kb (Ioannou *et al.*, 1994)) was screened by hybridization to heparanase cDNA probes. We identified five independent PAC genomic clones that contained overlapping human *HEP* gene segments. We mapped the *HEP* gene encoding heparanase to a single locus on chromosome 4q21 (Figure 3) by fluorescent *in situ* hybridization of metaphase chromosomes from human peripheral blood leukocytes. No hybridization signals were observed in other chromosomes. The chromosomal assignment was confirmed by performing two-color FISH analysis using a probe specific for the centromere of chromosome 4 in conjunction with the heparanase-specific probe (not shown). A total of 80 metaphase cells were analyzed with 77 (96%) demonstrating specific labeling. The murine *HEP* gene was localized to the E3-E5 region of mouse chromosome 5, which is syntenic to the centromere-proximal arm of human chromosome 4.

Heparanase expression in human tissues

Northern hybridization was performed to identify heparanase expression in various tissues and cell lines. A moderately abundant heparanase mRNA transcript, approximately 0.92 kb in size, was detected by a 3′ heparanase probe in all tissues examined (Figure 4A). However, placental tissues, which express abundant heparanase activity, contained 1.8 kb and 5.0 kb heparanase transcripts, which are large enough to encode a putative heparanase precursor protein and appear to be upregulated relative to the 0.92 kb transcript (Figure 4A). Trace amounts of the 1.8 kb transcript can also be visualized in the other tissues upon longer exposure, compatible with low-level heparanase expression, which might contribute metabolic turnover of cell-associated heparan sulfate within the endosomal-lysosomal compartment of cells expressing endogenous heparan sulfate proteoglycans, as suggested by Yanagishita and Hascall (1992). Because heparanase activity has been linked to tumor metastasis, we analyzed heparanase expression

Fig. 3. The human *HEP* gene is located on chromosome 4q21. The gene encoding heparanase is located at a single locus on chromosome 4q21 (FITC-staining). The chromosomal assignment was confirmed by cohybridization with a chromosome 4 centromere-specific probe (Texas red staining). Chromosomes were visualized with DAPI.

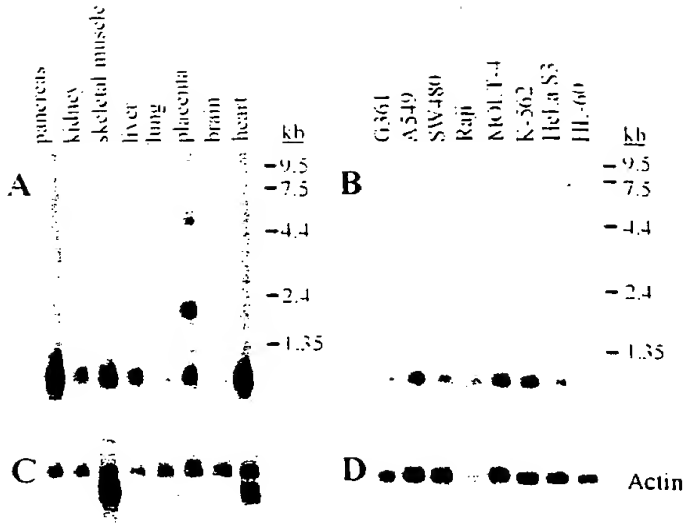

Fig. 4. Heparanase mRNA expression. Northern hybridization of poly(A)$^+$ mRNAs revealed heparanase-specific transcripts of 0.92 kb, 1.8 kb, and 5.0 kb in normal human tissues and in human cancer cell lines. (A) Heparanase expression in normal human tissues. (B) Heparanase expression in human tumor cell lines: melanoma G361, lung carcinoma A549, colorectal adenocarcinoma SW480, Burkitt's lymphoma Raji, lymphoblastic leukemia MOLT-4, chronic myelogenous leukemia K-562, cervical adenocarcinoma Hela S3, and promyelocytic leukemia HL-60. (C) β-actin expression in normal human tissues. (D) β-actin expression in human cancer cell lines.

within a panel of human cancer cell lines (Figure 4B). Transcripts of 0.92 kb, 1.8 kb, and 5.0 kb were also detected by the 3′ heparanase probe (Figure 4B). The 1.8 kb transcript was distinctly present in each cell line examined, as was the 5.0 kb transcript except in Raji and HL-60. However, in all cases, the 0.92 kb 3′-transcript was the most abundant mRNA species found. The 0.92 kb transcript detected in steady-state RNA populations by the 3′ heparanase probe may represent a stable but nonfunctional mRNA species, as the heparanase open reading frame exceeds this transcript size. However, an alternative-splice variant has not been ruled out. Alternative splicing or polyadenylation may produce the 5.0 kb transcript.

Localization of heparanase in human placental tissues

Because we found differences in heparanase expression in placenta, and because placenta tissue is an abundant source of heparanase activity, we sought to locate heparanase protein in human placenta. Human placenta obtained by Cesarean section was stained with either anti-heparanase (Hep1.1A) or anti-heparan sulfate (HepSS-1) monoclonal antibodies and then with FITC-conjugated anti-mouse IgM antibodies. Heparanase expression was evident in both extravillous trophoblast cells, which form the interface between fetal and maternal decidual tissues, and in syncytiotrophoblasts of the floating villi, which separate maternal and fetal blood supplies (Figure 5A,C). Diffuse heparanase staining was observed within villi cytotrophoblasts (Figure 5C). Intense heparanase antibody staining occurs in or near endothelial cells lining fetal arteries and capillaries within the villi (Figure 5C). Similar heparanase staining patterns were observed using rabbit anti-heparanase polyclonal antibodies (data not shown). Placenta stained with antibody preparations that had been immunodepleted were negative (not shown). We also localized heparan sulfate in placental tissues using an anti-heparan sulfate primary antibody, HepSS-1 (Figure 5D). Intense heparan sulfate deposition surrounds large fetal arteries, where heparan sulfate proteoglycans, notably perlecan, are found in the extracellular matrix basement membranes. Much less intense heparan sulfate staining was visible within the trophoblast cells lining fetal villi.

Heparanase expression in immune and inflammatory disease

Heparanase and heparan sulfate were located in tissues from porcine organs undergoing rejection following xenotransplantation into baboons (Platt, 1997). In organ transplantation, hyperacute rejection mediated by anti-donor antibody and complement is associated with platelet aggregation and release of granular contents with concomitant endothelial damage (Platt *et al.*, 1990b; Platt, 1996; Daniels and Platt, 1997; Platt, 1997). Using an *in vitro* model for hyperacute rejection, we have found that heparan sulfate is shed from porcine endothelial cells upon exposure to human serum, a source of xenoreactive antibodies and complement (Platt *et al.*, 1990b; Ihrcke and Platt, 1996). Similar vascular injury to endothelial cells can occur *in vivo*, where ~50% of metabolically labeled glycosaminoglycan chains are lost upon reperfusion of the donor organ within the recipient animal, and that administration of nonanticoagulant heparin can prevent both release of the glycosaminoglycan molecules and prolong graft survival (Stevens *et al.*, 1993).

We have postulated that inflammatory conditions induce both the release of platelet heparanase and activation of heparanase catalytic activity by lowering the pH of the vascular microenvironment (Ihrcke *et al.*, 1998). To examine this hypothesis *in vivo*, we analyzed porcine hearts undergoing hyperacute rejection for platelet aggregation, heparanase expression, and loss of vascular heparan sulfate. Blood vessels in a normal porcine heart are devoid of platelet aggregates, as

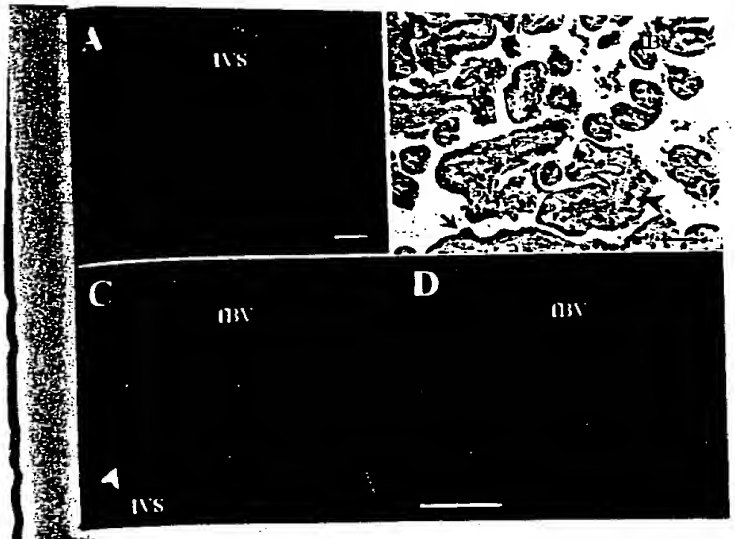

Fig. 5. Heparanase expression in human placental tissue. Heparanase protein was detected in tissues by indirect immunofluoresence using affinity-purified FITC-conjugated goat anti-mouse IgM antibodies to localize the primary Hep1.1A anti-heparanase antibody. Heparan sulfate glycosaminoglycans were also localized by indirect immunofluorescence using FITC-conjugated secondary antibodies to detect the primary murine IgM antibody HepSS-1. (A) Heparanase localization in extravillous trophoblasts in placental anchoring villi. Erythrocytes are visualized by their autofluorescence. (B) Placental H&E section showing placental tissue architecture: syncytiotrophoblast knots are observed by clustered nuclei (arrow), cytotrophoblasts demarcate the fetal interface with the maternal blood supply (arrowhead). IVS, intervillous space containing maternal blood; fBV, fetal blood vessels. (C) Heparanase is located in or near the endothelial cells lining fetal blood vessels in the chorionic villi. Heparanase is also found in cytotrophoblasts lining the villi (arrowhead). (D) Chorionic villi frozen section adjacent to that shown in (C) reveals a continuous ring of heparan sulfate surrounding fetal blood vessels. Scale bars: (A), 25 μm; (B), 40 μm; (C) and (D), 45 μm.

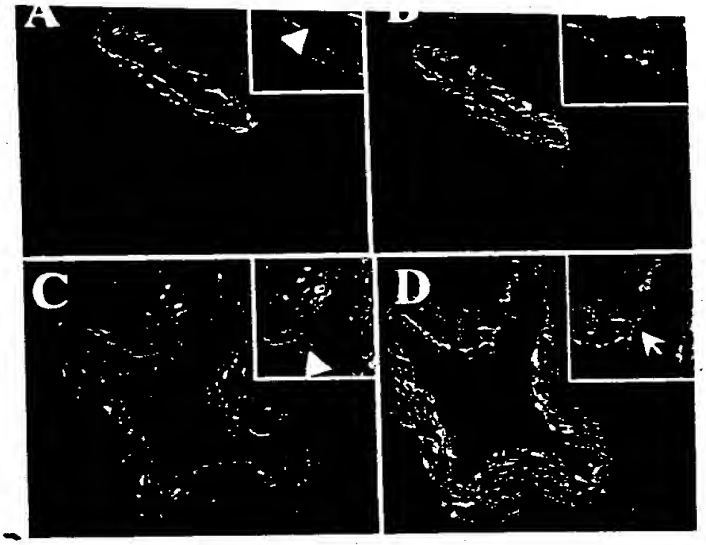

Fig. 6. Platelet heparanase is released within the vascular lesions of hyperacutely-rejecting organs upon xenotransplantation. Heparanase and heparan sulfate glycosaminoglycans were localized in porcine cardiac tissues by indirect immunofluorescence using FITC-conjugated secondary antibodies to detect Hep1.1A or HepSS-1 primary antibodies. The underlying extracellular matrix was counterstained using rhodamine-conjugated rabbit GBM50 anti-basement membranes antibodies. (A) Normal hearts contain heparanase within subendothelial matrices surrounding blood arteries. Inset, Heparanase does not appear to be present within blood vessel lumina in normal blood vessels (arrowhead). (B) Adjacent normal tissue section stained reveals heparan sulfate deposition in arteries and along basement membranes surrounding the myofibrils. Inset, Heparan sulfate staining extends up to the lumen of the blood vessel, including deposition on the endothelial cell surface. (C) Transplanted porcine heart undergoing hyperacute rejection shows focal deposition of heparanase on the luminal blood vessel surface. Hyperacute rejection is characterized pathologically by interstitial hemorrhaging, platelet aggregation, and vascular swelling. Inset, Higher magnification view showing heparanase deposition on the luminal blood vessel surface (arrowhead). Several nucleated cells can also be observed adhering to the blood vessel wall and appear to be transversing the endothelial cell border. (D) Adjacent tissue section shows loss of heparan sulfate from the luminal blood vessel surface. Inset, The underlying basement membrane can be seen exposed at multiple sites along the luminal blood vessel surface (arrow), and is especially prominent in the vicinity of heparanase deposition. Magnification 400x, insets 630x; scale bar, 50 μm.

evidenced by the lack of immunostaining with anti-human CD9, which recognizes primate platelets but no pig structures. Heparanase was observed with the subendothelial smooth muscle layer surrounding blood arteries in normal hearts (Figure 6A), but heparanase was not found on the luminal blood vessel surface (inset, Figure 6A). Normal tissues contained abundant heparan sulfate deposition within extracellular matrices surrounding blood vessels, extending up to the endothelial cell surface (inset, Figure 6B). However, when we examined tissues from hyperacute rejecting hearts, dense platelet aggregates were present in blood vessel lumen (not shown) and focal heparanase deposition was found on endothelial cell surfaces (Figure 6C). We asked if loss of heparan sulfate was correlated with the presence of heparanase in inflamed tissues. Examination of adjacent tissue sections demonstrated heparanase deposition (Figure 6C inset) on the luminal face of the blood vessel, which was coincident with loss of endothelial cell heparan sulfate staining (Figure 6D, inset arrow). Close inspection of the blood vessel surface revealed several nucleated cells, which appear to be transversing the endothelial cell boundary (inset, Figure 6C). These observations are consistent with heparanase activation *in vivo* in hyperacute organ rejection, and that heparanase activity might contribute to loss of vascular integrity, leading to the demise of organ transplants.

Discussion

Heparan sulfate metabolism is a dynamic process which is thought to influence many facets of development and tissue homeostasis. Loss of heparan sulfate from cell surfaces can disrupt interactions between adjacent cells, perturbing the local homeostatic cellular environment and inducing multiple cellular responses until a new equilibrium is reached. We show here that mature tissues, particularly those of the vascular system, are poised to respond immediately to changes within local microenvironments by the constitutive presence of heparanase. Our finding of heparanase within quiescent tissues obviates the temporal lag required for *de novo* synthesis and, during inflammatory episodes, can amplify the local response by attracting leukocytes to the site of damage and promote

diapedesis. This finding has important implications regarding the regulation of heparanase such that inadvertent activation is avoided, the region of heparanase activity is constrained, and the duration of heparanase activation is limited to prevent systemic damage.

The heparanase cDNA sequence we report is identical to the sequence recently reported by Vlodavsky *et al.* (1999) and Hulett *et al.* (1999); however, we report, here, differences in the tissue expression of heparanase protein that could impact on its physiological role(s). Vlodavsky *et al.* (1999) report localization of heparanase protein in primary or metastatic tumor tissues where heparanase might contribute to the degradation of extracellular matrices and, thereby, contribute to the dissemination of the tumor cells. However, heparanase mRNA and protein were not detected in normal tissues. In contrast, Northern hybridization data, shown here, suggests normal human tissues do express low steady-state levels of the 1.8 kb transcript, which is upregulated in placental tissues where abundant heparanase activity is found. Increased steady-state levels of this 1.8 kb transcript were also found in several human cancer cell lines, as shown here and in lymphoid tissues, such as bone marrow and peripheral blood leukocytes (Hulett *et al.*, 1999). Under physiological conditions, heparanase activity may be limited to acidified membrane compartments, such as the lysosome, where heparan sulfate proteoglycans may be degraded to achieve steady-state levels. Under conditions of inflammation, heparanase may be secreted by platelets or leukocytes into local blood vessel lumen, compromising vascular integrity and allowing the passage of blood-borne cells into interstitial spaces. In addition, inactive forms of heparanase protein may be tethered to extracellular matrices. We report, here, finding heparanase protein in subendothelial locations in both normal tissues and tissues undergoing humoral-induced vascular rejection episodes. Antibodies against N-terminal peptides found in the precursor domain did not recognize heparanase protein within placental or heart tissues in immunofluorescence experiments, suggesting that the tethered heparanase molecules are not unprocessed precursors but might be mature protein (data not shown). We would postulate that heparanase may be activated in inflamed tissue as local pH decreases, as discussed below. The loss of endothelial cell heparan sulfate in the latter tissues, but not the former, is consistent with heparanase activation under inflammatory conditions.

The anti-heparanase antibodies used in our studies recognized peptide epitopes of the mature active protein, and were shown to specifically recognize denatured heparanase by Western immunoblots, and native platelet heparanase by ELISA. Moreover, by employing a stringent assay to measure inhibition of heparanase activity, we show the anti-heparanase antibodies recognize a significant fraction of active heparanase. To our knowledge, this is the first report describing antibody reagents that affect heparanase activity.

Given the detection of heparanase protein in normal tissues and the pathophysiologic consequences, were heparanase to be active, it would not be surprising that tight regulatory mechanisms control enzyme activity. We have postulated that the activity of expressed heparanase protein is regulated by microenvironmental conditions, particularly by pH. Heparanase binds to but does not degrade heparan sulfate glycosaminoglycans at physiological pH (Gilat *et al.*, 1995; Ihrcke *et al.*, 1998). Heparanase endoglycosidase activity is optimal between pH 5.0 and 6.5; however, the enzyme is much less active when the pH is above 7.0 (Oosta *et al.*, 1982; Gilat *et al.*, 1995; Freeman and Parish, 1998; Ihrcke *et al.*, 1998). Heparanase activity progressively decreases at neutral pH, but can be reactivated under acidic conditions (Ihrcke *et al.*, 1998). This property confers an important regulatory mechanism that may confine heparanase action to injured vascular sites, where inflammatory conditions lower the pH and are, thus, favorable for heparanase activity, thereby preventing systemic activation and inadvertent damage to distal endothelium. We have demonstrated, here, in pathophysiological findings of hyperacute rejection, where inflammatory vascular lesions abound, that heparanase becomes activated on endothelial surfaces with the concomitant loss of heparan sulfate and vascular integrity.

Additional mechanisms may exist to promote or inhibit heparanase activity in normal tissues and during development. Heparanase mRNA is expressed in many human tissues and immortalized tumor cell lines, but the pattern of expression differs, qualitatively, in tissues where abundant heparanase activity has been reported, suggesting posttranscriptional regulatory mechanisms act upon heparanase mRNA stability. The most abundant heparanase transcript found in steady-state mRNA populations appears to be too small to encode the mature protein product and lacks methionine initiation codons in the proper open reading frame. Regulation of heparanase activity may also involve competing protein interactions by blocking enzyme access to its substrate, as may occur by the cell surface protein heparan sulfate/heparin-interacting protein (HIP), first identified in uterine epithelial cells and, subsequently, found to be expressed in various epithelial and endothelial cells (Liu *et al.*, 1997). HIP binds to the same oligosaccharide sequence as antithrombin III (Liu *et al.*, 1997) and antagonizes heparan sulfate digestion by heparanase, presumably by competing for the same binding recognition site in the glycosaminoglycan chain (Marchetti *et al.*, 1997). Expression of competing heparan sulfate-binding proteins may, in part, explain why abundant heparanase proteins are present in placental tissues, but adverse pathophysiological episodes normally do not occur during gestation. However, this notion raises the possibility that some complications in pregnancy, such as defective placenta formation in preeclampsia or abnormal maternal bleeding episodes, could be, in part, attributed to defective heparanase regulation.

The development of molecular tools, as described here, to study heparanase expression and regulation will no doubt contribute to our understanding of how heparanase functions during development, in tissue homeostasis and in disease. The ability to overexpress recombinant heparanase proteins will allow detailed investigation of the structural basis governing the pH-dependence of heparanase catalytic activity. Such knowledge can lead to the rational design of molecules, which may block structural transitions or sterically-hinder the heparanase catalytic active site or ligand-binding domain, thereby precluding heparanase digestion of heparan sulfate, and may be beneficial as a therapeutic intervention in disease states.

Materials and methods

Identification of heparanase cDNA clones

Heparanase cDNA clones were identified by searching translated dbEST databases for human cDNAs capable of encoding platelet heparanase peptides LYGPDVGQPRRK, NVDDQTLPPLMEK, and LRVYLHCTNTDNPRYK (Gonzalez-Stawinski *et al.*, 1999) using the BLAST (Basic local alignment search tool (Altschul *et al.*, 1990)) computer algorithm. Three positive clones were found within the Soares placental cDNA library, identified as ID 257548, ID 257583, and ID 260138, and are among the cDNA collection deposited by the I.M.A.G.E. Consortium (Lennon *et al.*, 1996: Lawrence Livermore National Laboratory).

Cell culture

The human CHRF-288 megakaryoblast cell line, (Fugman *et al.*, 1990), was cultured at 37°C in Fischer's medium (Life Technologies, Grand Island, NY) supplemented with 10% fetal bovine serum (FBS), 100 U/ml penicillin-streptomycin, 2 mM L-glutamine, and 1 mM sodium pyruvate (Life Technologies).

Heparanase activity assays

Heparanase activity was assayed using ^{3}H-heparan sulfate-Sepharose beads, prepared as described previously (Ihrcke *et al.*, 1998). Washed platelets were resuspended in heparanase assay buffer (0.1 M sodium acetate, pH 5.0, 0.1 mg/ml bovine serum albumin, 0.01% Triton X-100; and protease inhibitors (0.5 mM phenylmethylsulfonyl fluoride, 10 μg/ml leupeptin, and 10 μg/ml pepstatin A), and subjected to several freeze–thaw cycles (−70°C/37°C). Clarified lysates were obtained by centrifugation at 34,000 × *g* for 30 min at 4°C. Platelet lysate, 100 μg protein, was added to 350 μl heparanase buffer, 50 μl ^{3}H-heparan sulfate-Sepharose beads equilibrated in the same buffer, and incubated at 37°C for 4 h. Release of ^{3}H-heparan sulfate was quantitated by measuring the radioactivity in supernatant fractions by scintillation counting. Assays were performed in triplicate and each experiment was performed at least twice on separate days. Activity is reported as the mean amount of radioactivity (c.p.m.) released per 100 μg protein. Protein concentrations were determined by the detergent-compatible Lowry protein assay (Bio-Rad, Hercules, CA) using BSA as standards.

Generation of anti-heparanase antibodies

Mice were immunized with a synthetic peptide conjugate (Bio-Synthesis, Lewisville, TX) KLRVYLHCTNTDN (amino acids 430–442) found within human heparanase. Responding mice were sacrificed and their splenic B cells fused with FO-SP2/O myeloma cells (Galfré and Milstein, 1981). Hybridoma lines secreting anti-heparanase antibodies were identified by ELISA and cloned by limiting dilution. Isotype determination was performed using goat anti-mouse γ-chain specific or goat anti-mouse μ-chain specific antibodies (Sigma Chemicals, St. Louis, MO) in ELISA reactions. Rabbits were immunized using the same peptide conjugate to generate polyclonal antibodies. Additional peptides CKYGSIPPDVEEK (amino acids 128–140) and TKVLMASVQGSKRRK (amino acids 417–431) were coupled to maleimide-activated keyhole limpet hemocyanin carrier protein (Pierce) and used to immunize mice, as described above. To demonstrate the specificity of the anti-heparanase monoclonal and polyclonal antibodies, competitive ELISA assays were performed with fixed concentrations of platelet extract and anti-heparanase antibody in PBS, 0.1% BSA with increasing amounts of the peptide KLRVYLHCTNTDN. Alkaline phosphatase–conjugated goat α-mouse IgM or goat α-rabbit IgG (diluted 1:1000 in PBS, 0.1% BSA) were used to detect primary immune complexes, followed by incubation with disodium p-nitrophenyl phosphate (Sigma Chemicals). Antibody binding was quantitated by measuring the absorbance at 405 nm. Western immunoblotting was performed by resolving human platelet extracts on 10–20% gradient denaturing polyacrylamide gels, followed by transfer to PVDF membranes. Goat α-rabbit IgG or rabbit α-mouse IgM alkaline phosphatase-conjugated antibodies were used to detect primary immune complexes with NBT/BCIP reagents. To test for the ability of antibodies to inhibit heparanase activity, human platelet extracts (100 μg) were incubated in the presence of anti-heparanase monoclonal antibodies (100 μg) for 3 h, at room temperature, under conditions which are permissible for catalytic activity, (0.1 M sodium acetate, pH 6.5, 0.1 mg/ml bovine serum albumin, 0.01% Triton X-100; and protease inhibitors). Aliquots were removed to tubes containing immobilized ^{3}H-heparan sulfate–Sepharose beads and were incubated 1.5 h further in the presence of protein A/G agarose beads, to which goat anti-mouse μ-chain antibodies had been coupled. Following incubation, the beads were pelleted and the supernatant removed for assay of heparanase activity. Immunoglobulin isotype controls, 2C18, which recognizes human complement factor C5a, and mock-treated protein A/G beads, were tested likewise.

Chromosomal localization of the human heparanase gene

Fluorescence *in situ* hybridization mapping of human metaphase chromosomes was performed using digoxigenin dUTP-labeled DNA probes, which were combined with sheared human DNA and hybridized to normal metaphase chromosomes in a solution containing 50% formamide, 10% dextran sulfate, and 20× SSC. Specific hybridization signals were detected by incubating the hybridized slides in fluoresceinated anti-digoxigenin antibodies followed by counterstaining with DAPI.

Northern blot hybridization

Northern blots containing 2 μg poly(A)+ mRNA from normal human tissues or from a variety of human cancer cell lines (Clontech, Inc., Palo Alto, CA) were hybridized to a 475-bp ^{32}P-labeled probe, derived from the 3′ end of the human heparanase cDNA (coordinates 1004–1479), which was generated by PCR-amplification using primers Hep1, 5′-CTGGCAAGAAGGTCTGGTT-3′, and Hep3, 5′-GACA-GATTTGGAAAGTAATCC-3′. Probes were radiolabeled to a specific activity of 1.0×10^{9} c.p.m./μg by random-hexamer primer extension (Boehringer Mannheim, Indianapolis, IN) and [α-^{32}P]dCTP (Amersham, Arlington Heights, IL). Hybridization was performed at 68°C in ExpressHyb solution (Clontech). Blots were washed twice in 2× SSC, 0.05% SDS at room temperature, then twice in 0.1× SSC, 0.1% SDS at 50°C for 30 min, and exposed to Kodak XAR x-ray film. The blots were subsequently stripped and reprobed with a human β-actin probe for normalization of the amount of RNA loaded per lane. Blots were exposed to film for 90 h with an intensifying screen

at –80°C to detect heparanase expression, whereas exposure times for detecting β-actin were 3 h.

RNA preparation, RT-PCR, and 5′-RACE (rapid amplification of DNA ends)

Total RNA was prepared from CHRF-288 cells by the guanidinium thiocyanate method (Chomczynski and Sacchi, 1987). Heparanase cDNAs were synthesized using Hep3 antisense primer and AMV reverse transcriptase (Boehringer Mannheim) and 3′poly(dA)-tailed with dATP and TdT. Two rounds of nested PCR amplification were performed with Expand PCR polymerase (Boehringer Mannheim) using antisense primers Hep4, 5′-GATCGAAGTTTTCATCCAC-3′, and Hep5, 5′ GTGATGCCATGTAACTG-3′, and oligo(dT) or an anchor primer provided by the manufacturer (Boehringer Mannheim). Alternatively, human placental cDNA (Clontech) was utilized as the starting material for nested PCR amplification and used high temperature "touchdown" PCR cycling conditions in a Perkin-Elmer GeneAmp9600 thermocycler (94°C, 30 sec; 5 cycles at 94°C for 5 sec, 72°C for 4 min; 5 cycles at 94°C for 5 sec, 70°C for 4 min; 25 cycles at 94°C for 5 sec, 68°C for 4 min). Heparanase clones were identified by producing a diagnostic PCR product of 235 bp using a Hep7 (5′-GGCACGAGGAGGCAATGAACCT-3′)-Hep5 primer pair. The nucleotide sequence of positive clones was determined by the dideoxynucleotide chain termination method.

Indirect immunofluorescence

Representative specimens of human placenta (obtained by caesarian section), normal porcine heart tissue, and porcine hearts undergoing hyperacute rejection after xenotransplantation into baboon recipients, were snap-frozen in precooled isopentane and stored at –85°C until cyrosectioning. Tissue sections (4 μm) were cut using a Leica CM 3050 cryostat and mounted on positively charged microscope slides, briefly heat-fixed, and stored at –85°C. Sections were acetone-fixed 10 min at 4°C, and postfixed for 2 min in Tris-buffered 1% paraformaldehyde, 1 mM EDTA, pH 7.2. Formalin-fixed, paraffin-embedded tissue sections were prepared by placing tissue specimens in 10% neutral-buffered formalin, pH 7.2, for ⩾8 h at room temperature, after which samples were processed and embedded into paraffin blocks. Tissue sections (4 μm) were obtained using a rotary microtome (model 2155, Leica) and mounted onto positively charged microscope slides. Primary antibodies were diluted and applied to tissue sections including monoclonals Hep1.1A (mouse IgM anti-human heparanase), HepSS-1 (mouse IgM anti-heparan sulfate, Seikagaku, Tokyo), and BA-2 (mouse IgG anti-CD9). Secondary fluorochrome-labeled antibodies were used to detect binding by the primary antibodies. Affinity-purified, FITC-conjugated goat F(ab′)2 anti-mouse IgM (1:100) or anti-mouse IgG (1:200; Cappel-ICN, Aurora, OH) was applied to the primary antibody-stained tissue sections. A third layer of FITC-conjugated rabbit F(ab′)2 anti-goat IgG (Cappel-ICN), diluted 1:50, and rhodamine-conjugated rabbit anti-human basement membrane GBM50 (diluted 1:100) were applied to tissue samples. All fluorochrome antibodies were preabsorbed with human and porcine serum prior to use. Sections were counterstained/coverslipped with Vectashield-DAPI (Vector Laboratories, Burlington, CA) for detection of nuclei and stored in the dark at 4°C until microscopic evaluation using a fluorescence research microscope (Leica DMRD). Photographic images were obtained utilizing a CCD digital camera (SPOT II, Diagnostic Instruments, Sterling Heights, MI).

Acknowledgments

Sequences have been deposited in GenBank (accession number AF084467). We are grateful to Dr. Thomas Gaffey for providing human placental tissues and for stimulating discussions. We thank Kim Butters, Karen Lien, Robert Holzknecht, and Karisha Kuypers for excellent technical help. This work was supported by grants from the National Institutes of Health (J.L.P.) and Duke Comprehensive Cancer Center-American Cancer Society Institutional Award (L.A.D.).

Abbreviations

cDNA, complementary DNA; c.p.m., counts per minute; DAPI, 4,6–diamidino-2-phenylindole-dihydrochloride; dbEST, database of expressed sequence tags; ELISA, enzyme-linked immunosorbent assay; FISH, fluorescent *in situ* hybridization; H&E, hexatoxylin & eosin; HSE, heparan sulfate endoglycosidase; I.M.A.G.E., Integrated Molecular Analysis of Genomes and their Expression; kb, kilobase; kDa, kilodalton; nt, nucleotides; ORF, open reading frame; PCR, polymerase chain reaction; RACE, rapid amplification of DNA ends; SDS, sodium dodecyl sulfate; TdT, terminal deoxynucleotide transferase.

References

Altschul,S.F., Gish,W., Miller,W., Myers,E.W. and Lipman,D.J. (1990) Basic local alignment search tool. *J. Mol. Biol.*, **215**, 403–410.

Bernfield,M., Kokenyesi,R., Kato,M., Hinkes,M.T., Spring,J., Gallo,R.L. and Lose,E.J. (1992) Biology of the syndecans: a family of transmembrane heparan sulfate proteoglycans. *Annu. Rev. Cell. Biol.*, **8**, 365–393.

Brunner,G., Garilove,J., Rifkin,D.B. and Wilson,E.L. (1991) Phospholipase C release of basic fibroblast growth factor from human bone marrow cultures as a biologically active complex with a phosphatidylinositol-anchored heparan sulfate proteoglycan. *J. Cell Biol.*, **114**, 1275–1283.

Cardin,A.D. and Weintraub,H.J. (1989) Molecular modeling of protein-glycosaminoglycan interactions. *Arteriosclerosis*, **9**, 21–32.

Carson,D.D., DeSouza,M.M. and Regisford,E.G.C. (1998) Mucin and proteoglycan functions in embryo implantation. *Bioessays*, **20**, 577–583.

Cross,J.C., Werb,Z. and Fisher,S.J. (1994) Implantation and the placenta: key pieces of the development puzzle. *Science*, **266**, 1508–1518.

Chomczynski,P. and Sacchi,N. (1987) Single-step method of RNA isolation by acid guanidinium thiocyanate-phenol-chloroform extraction. *Anal. Biochem.*, **162**, 156–159.

Daniels,L.J. and Platt,J.L. (1997) Hyperacute xenograft rejection as an immunologic barrier to xenotransplantation. *Kidney Int.*, **51**, S28–S35.

Freeman,C. and Parish,C.R. (1998) Human platelet heparanase: purification, characterization and catalytic activity. *Biochem. J.*, **330**, 1341–1350.

Fridman,R., Lider,O., Naparstek,Y., Fuks,Z., Vlodavsky,I. and Cohen,I.R. (1987) Soluble antigen induces T lymphocytes to secrete an endoglycosidase that degrades the heparan sulfate moiety of subendothelial extracellular matrix. *J. Cell Physiol.*, **130**, 85–92.

Fugman,D.A., Witte,D.P., Jones,C.L.A., Aronow,B.J. and Lieberman,M.A. (1990) *In vitro* establishment and characterization of a human megakaryoblastic cell line. *Blood*, **75**, 1252–1261.

Galfré,G. and Milstein,C. (1981) Preparation of monoclonal antibodies: strategies and procedures. *Methods Enzymol.*, **73**, 3–46.

Gilat,D., Hershkoviz,R., Goldkorn,I., Cahalon,L., Korner,G., Vlodavsky,I. and Lider,O. (1995) Molecular behavior adapts to context: heparanase functions as an extracellular matrix-degrading enzyme or as a T-cell adhesion molecule, depending on the local pH. *J. Exp. Med.*, **181**, 1929–1934.

Platt,J.L. (1999) Partial sequence of human platelet heparitinase and dence of its ability to polymerize. *Biochim. Biophys. Acta*, **1429**, 431–438.
Goshen,R., Hochberg,A.A., Korner,G., Levy,E., Ishai-Michaeli,R., Elkin,M., de Groot,N. and Vlodavsky,I. (1996) Purification and characterization of placental heparanase and its expression by cultured cytotrophoblasts. *Mol. Human Reproduction*, **2**, 679–684.
Graham,L.D. and Underwood,P.A. (1996) Comparison of the heparanase enzymes from mouse melanoma cells, mouse macrophages and human platelets. *Biochemistry Mol. Biol. Int.*, **39**, 536–571.
Hileman,R.E., Fromm,J.R., Weiler,J.M. and Linhardt,R.J. (1998) Glycosaminoglycan–protein interactions: definition of consensus sites in glycosaminoglycan binding proteins. *Bioessays*, **20**, 156–167.
Hoogewerf,A.J., Leone,J.W., Reardon,I.M., Howe,W.J., Asa,D., Heinrikson,R.L. and Ledbetter,S.R. (1995) CXC chemokines connective tissue activating peptide-III and neutrophil activating peptide-2 are heparin/heparan sulfate-degrading enzymes. *J. Biol. Chem.*, **270**, 3268–3277.
Hulett,M.D., Freeman,C., Hamdorf,B.J., Baker,R.T., Harris,M.J. and Parish,C.R. (1999) Cloning of mammalian heparanase, an important enzyme in tumor invasion and metastasis. *Nature Med.*, **5**, 803–809.
Ihrcke,N.S. and Platt,J.L. (1996) Shedding of heparan sulfate proteoglycan by stimulated endothelial cells: evidence for proteolysis of cell surface molecules. *J. Cell Physiol.*, **168**, 625–637.
Ihrcke,N.S., Parker,W., Reissner,K.J. and Platt,J.L. (1998) Regulation of platelet heparanase during inflammation: role of pH and proteinases. *J. Cell Physiol.*, **175**, 255–267.
Ihrcke,N.S., Wrenshall,L.E., Lindman,B.J. and Platt,J.L. (1993) Role of heparan sulfate in immune system–blood vessel interactions. *Immunol. Today*, **14**, 500–505.
Ioannou,P., Amemiya,C., Garnes,J., Kroisel,P., Shizuya,H., Chen,C., Batzer,M. and de Jong,P. (1994) A new bacteriophage P1-derived vector for the propagation of large human DNA fragments. *Nature Genet.*, **6**, 84–89.
Ishai-Michaeli,R., Eldor,A. and Vlodavsky,I. (1990) Heparanase activity expressed by platelets, neutrophils and lymphoma cells releases active fibroblast growth factor from the extracellular matrix. *Cell Reg.*, **1**, 833–842.
Kim,C.H. and Broxmeyer,H.E. (1999) Chemokines: signal lamps for trafficking of T and B cells for development and effector function. *J. Leukocyte Biol.*, **65**, 6–15.
Kjellen,L. and Lindahl,U. (1991) Proteoglycans: structures and interactions. *Annu. Rev. Biochem.*, **60**, 443–475.
Kyte,J. and Doolittle,R.F. (1982) A simple method for displaying the hydropathic character of a protein. *J. Mol. Biol.*, **157**, 105–132.
Lennon,G., Auffray,C., Polymeropoulos,M. and Soares,M.B. (1996) the I.M.A.G.E. consortium: an integrated nuclear analysis of genomes and their expression. *Genomics*, **33**, 151–152.
Lindahl,U., Kusche-Gullberg,M. and Kjellén,L. (1998) Regulated diversity of heparan sulfate. *J. Biol. Chem.*, **273**, 24979–24982.
Liu,S., Zhou,F., Höök,M. and Carson,D.D. (1997) A heparin-binding synthetic peptide of heparin/heparan sulfate-interacting protein modulates blood coagulation activities. *Proc. Natl. Acad. Sci. USA*, **94**, 1739–1744.
Marchetti,D., Liu,S., Spohn,W.C. and Carson,D.D. (1997) Heparanase and a synthetic peptide of heparan sulfate-interacting protein recognize common sites on cell surface and extracellular matrix heparan sulfate. *J. Biol. Chem.*, **272**, 15891–15897.
Matzner,Y., Bar-Ner,M., Yahalom,J., Ishai-Michaeli,R., Fuks,Z. and Vlodavsky,I. (1985) Degradation of heparan sulfate in the subendothelial extracellular matrix by a readily released heparanase from human neutrophils: possible role in invasion through basement membranes. *J. Clin. Invest.*, **76**, 1306–1313.
Nakajima,M., Di Ferrante,D., Irimura,T., Di Ferrante,N. and Nicolson,G.L. (1983) Heparan sulfate degradation: relation to tumor invasive and metastatic properties of mouse B16 melanoma sublines. *Science*, **220**, 611–612.
Naparstek,Y., Cohen,I.R., Fuks,Z. and Vlodavsky,I. (1984) Activated T-lymphocytes produce a matrix-degrading heparan sulfate endoglycosidase. *Nature*, **310**, 241–244.
Oosta,G.M., Favreau,L.V., Beeler,D.L. and Rosenberg,R.D. (1982) Purification and properties of human platelet heparitinase. *J. Biol. Chem.*, **257**, 11249–11255.
Platt,J.L. (1996) The immunological barriers to xenotransplantation. *Crit. Rev. Immunol.*, **16**, 331–358.
Platt,J.L. (1997) Hyperacute xenograft rejection. In Cooper,D.K.C., (ed.), *Xenotransplantation*. Springer-Verlag, Heidelberg.
Platt,J.L., Trescony,P., Lindman,B.J. and Oegema,T.R. (1990a) Heparin and heparan sulfate delimit nephron formation in fetal metanephric kidneys. *Dev. Biol.*, **139**, 338–348.
Platt,J.L., Vercellotti,G.M., Lindman,B.J., Oegema,T.R.,Jr., Bach,F.H. and Dalmasso,A.P. (1990b) Release of heparan sulfate from endothelial cells: Implications for the pathogenesis of hyperacute rejection. *J. Exp. Med.*, **171**, 1363–1368.
Rosenberg,R.D., Shworak,N.W., Liu,J., Schwartz,J.J. and Zhang,L. (1997) Heparan sulfate proteoglycans of the cardiovascular system. *J. Clin. Invest.*, **99**, 2062–2070.
Salmivirta,M., Lidholt,K. and Lindahl,U. (1996) Heparan sulfate: a piece of information. *FASEB J.*, **10**, 1270–1279.
Sandbäck Pikas,D., Li,J.-p., Vlodavsky,I. and Lindahl,U. (1998) Substrate specificity of heparanases from human hepatoma and platelets. *J. Biol. Chem.*, **273**, 18770–18777.
Shimada,K. and Ozawa,T. (1987) Subendothelial extracellular-matrix heparan sulfate proteoglycan-degrading activity of human monocyte macrophages. *Heart Vessels*, **3**, 175–181.
Stevens,R.B., Wang,Y.L., Kaji,H., Lloveras,J., Dalmasso,A.B., Bach,F.H., Rubinstein,P., Sutherland,D.E.R. and Platt,J.L. (1993) Administration of nonanticoagulant heparin inhibits the loss of glycosaminoglycans from xenogeneic cardiac grafts and prolongs graft survival. *Transplant Proc.*, **25**, 382.
Stringer,S.E. and Gallagher,J.T. (1997) Heparan sulphate. *Int. J. Biochem. Cell Biol.*, **29**, 709–714.
Villanueva,G.B., Nakajima,M. and Nicolson,G.L. (1989) Heparin derivatives as inhibitors of heparanase from metastatic melanoma cells. *Ann. N.Y. Acad. Sci.*, **556**, 496–498.
Vlodavsky,I., Eldor,A., Bar-Ner,M., Friedman,R., Cohen,I.R. and Klagsbrun,M. (1988) Heparan sulfate degradation in tumor cell invasion and angiogenesis. *Adv. Exp. Med. Biol.*, **233**, 201–210.
Vlodavsky,I., Eldor,A., Haimovitz-Friedman,A., Ishai-Michaeli,R., Lider,O., Naparstek,Y., Cohen,I.R. and Fuks,Z. (1992) Expression of heparanase by platelets and circulating cells of the immune system: possible involvement in diapedesis and extravasation. *Invasion Metastasis*, **12**, 112–127.
Vlodavsky,I., Friedman,Y., Elkin,M., Aingorn,H., Atzmon,R., Ishai-Michaeli,R., Bitan,M., Pappo,O., Peretz,T., Michal,I., Spector,L. and Pecker,I. (1999) Mammalian heparanase: gene cloning, expression and function in tumor progression and metastasis. *Nature Med.*, **5**, 793–802.
Weiss,L., Orr,F.W. and Honn,K.V. (1988) Interactions of cancer cells with the microvasculature during metastasis. *FASEB J.*, **2**, 12–21.
Wrenshall,L.E., Cerra,F.B., Carlson,A., Bach,F.H. and Platt,J.L. (1991) Regulation of T lymphocyte responses by heparan sulfate. *J. Immunol.*, **147**, 455–459.
Wrenshall,L.E., Carlson,A., Cerra,F.B. and Platt,J.L. (1994) Modulation of cytolytic T-cell responses by heparan sulfate. *Transplantation*, **57**, 1087–1094.
Yanagishita,M. (1992) Glycosylphosphatidylinositol-anchored and core protein intercalated heparan sulfate proteoglycans in rat ovarian granulosa cell have distinct secretory, endocytic and intracellular degradative pathways. *J. Biol. Chem.*, **267**, 9505–9511.
Yanagishita,M. and Hascall,V.C. (1992) Cell surface heparan sulfate proteoglycans. *J. Biol. Chem.*, **267**, 9451–1992.